Nanoparticle dynamics in semidilute polymer solutions: Rings versus linear chains

Renjie Chen, Shivraj B. Kotkar, Ryan Poling-Skutvik, Michael P. Howard, Arash Nikoubashman, Jacinta C. Conrad, and Jeremy C. Palmer

Citation: Journal of Rheology **65**, 745 (2021); doi: 10.1122/8.0000223
View online: https://doi.org/10.1122/8.0000223
View Table of Contents: https://sor.scitation.org/toc/jor/65/4
Published by the The Society of Rheology

Nanoparticle dynamics in semidilute polymer solutions: Rings versus linear chains

Renjie Chen,[1] Shivraj B. Kotkar,[1] Ryan Poling-Skutvik,[2] Michael P. Howard,[3] Arash Nikoubashman,[4] Jacinta C. Conrad,[1,a)] and Jeremy C. Palmer[1,b)]

[1]*Department of Chemical and Biomolecular Engineering, University of Houston, Houston, Texas 77204*
[2]*Department of Chemical Engineering, University of Rhode Island, Kingston, Rhode Island 02881*
[3]*Department of Chemical Engineering, Auburn University, Auburn, Alabama 36849*
[4]*Institute of Physics, Johannes Gutenberg University Mainz, Staudingerweg 7, 55128 Mainz, Germany*

(Received 8 January 2021; final revision received 18 March 2021; published 21 June 2021)

Abstract

We study the dynamics of nanoparticles in semidilute solutions of ring and linear polymers using hybrid molecular dynamics–multiparticle collision dynamics simulations. The dynamics of the monomers, the polymer centers-of-mass, and the nanoparticles coincide for these two architectures for solutions of the same monomer concentration. The long time diffusivities of the nanoparticles follow the predictions of a polymer coupling theory [Cai *et al.*, Macromolecules **44**, 7853–7863 (2011)], suggesting that nanoparticle dynamics are coupled to segmental relaxations for both polymer architectures examined here. At intermediate time scales, the nanoparticle dynamics are characterized by subdiffusive exponents, which markedly deviate from coupling theory and closely follow those of the polymers. Instead, the nanoparticle dynamics are strongly coupled to the polymer center-of-mass motions for both architectures, rather than to their segmental dynamics. The presence of ring concatenations does not affect the long-time diffusivity of the nanoparticles but leads to a slight decrease in the subdiffusive exponents of the nanoparticles and the polymer center-of-mass. https://doi.org/10.1122/8.0000223

I. INTRODUCTION

Transport of nanoparticles (NPs) in polymer solutions appears in a variety of practical settings, including processing of polymer nanocomposites [1–3], hydrocarbon exploration and production [4], and drug delivery [5–8]. Control over the dispersion of NPs in these settings requires fundamental studies aimed at understanding the factors influencing NP transport in polymer solutions. In a Newtonian fluid, NPs diffuse according to the solution viscosity following the Stokes–Einstein (SE) relationship. In a polymer solution, NPs that are larger than characteristic solution length scales, e.g., the polymer's radius of gyration or mesh size, couple dynamically to the bulk solution viscoelasticity. This size regime can be described accurately via the generalized Stokes–Einstein relationship, which is widely applied in microrheology [9,10]. When NPs are comparable in size or smaller than the typical solution length scales, however, the polymer solution cannot be treated as a homogeneous medium anymore so that the continuum assumption underlying the framework of microrheology cannot be applied. Indeed, many experiments report dynamics of NPs that are faster than predicted from the bulk viscosity [11–15]. As a result, theoretical [16–20] and computational [21–26] approaches have been extensively employed to explore the factors controlling NP diffusion in polymer solutions.

Most studies of NP transport to date have focused on solutions of linear polymers, which are readily synthesized. Polymers of other architectures, however, are widely found in natural and engineered systems, but their role in NP transport has received considerably less attention. For example, circular architectures have been observed in biologically relevant macromolecules such as DNA [27–29], and ring polymers in a melt or solution are considered good models of chromatin [30–33]. The closed conformations of ring polymers can lead to structural and dynamical properties that strongly differ from those of linear chains [28–31,34–41]. These differences remain incompletely understood theoretically because free ends, which are absent in ring polymers, are critical to many well-established models for describing chain relaxation processes, e.g., the reptation model for linear chains [42] and the back-folding model for branched polymers [43]. As a result, open questions remain regarding the nature of relaxations in ring polymers and how they may influence transport processes in solutions and melts.

It has been suggested that both statics and dynamics of ring polymers are self-similar [32], that is, similar conformations and motions are observed in any part of the chain due to its circular symmetry. Early theories [44–46] for describing the conformations and motions of ring polymer melts were inspired by the de Gennes reptation model of a linear polymer [42], which describes motions of the entire molecule in terms of motions of "diffusing kinks" along the chain. Flexible ring polymers exhibit relatively compact structures

Note: This paper is part of the special issue on Ring Polymers.

[a)]Electronic mail: jcconrad@uh.edu
[b)]Author to whom correspondence should be addressed; electronic mail: jcpalmer@uh.edu

compared to linear chains and frequently interpenetrate due to the low energy barrier associated with transitioning to more open configurations [30]. The radius of gyration for linear chains in melts scales as $R_g \sim N_m^{\nu}$ with number of monomers N_m and Flory exponent $\nu = 1/2$. For ring polymers, simulations [30] indicated an initial scaling of $N_m^{1/2}$ for small N_m, followed by an intermediate regime with $N_m^{2/5}$ scaling, and then an eventual crossover to $N_m^{1/3}$ scaling in the large-size limit, supporting the crumpled globule picture [47] with $\nu = 1/3$. In solutions, by contrast, simulations predict similar ν values for ring and linear polymers (≈ 0.60 and 0.58, respectively) in a good solvent, but suggest that the exponent ν for ring polymers decreases more slowly as solvent quality worsens [39].

Theories for ring polymer dynamics in melts have been proposed based on the diffusing kinks picture [48] and Rouse dynamics [49]. Although the diffusion coefficient of a ring polymer scales with contour length in a similar way to that of a reptating linear chain [44–46,48], the relaxation modes are quite different due to the absence of free ends. Whereas linear chains readily form entanglements at high concentrations and molecular weights, ring polymers avoid or delay entanglements due to their lack of free ends [48]. As a result, ring polymers relax significantly faster than linear polymers of the same molecular weight [35].

Concatenation defects are a second unique feature of ring polymers. Concatenated rings are irreversibly linked and thus never separate from each other due to their permanent topological constraints. For nonconcatenated rings, by contrast, no permanent constraints exist [50], and deviations from linear chain behavior arise solely from their closed conformations. Although not as widely studied, the effects of interlinking on polymer properties in melts [51,52] and solvents of varying quality [53,54] have also been explored.

Inspired by the unique structural and dynamical properties of ring polymers, recent studies have begun to investigate NP transport in entangled ring polymer systems. Molecular dynamics (MD) simulations of NPs in entangled melts of nonconcatenated ring polymers [33,55] revealed that NP motions are not as strongly suppressed as in melts of linear chains. The faster NP dynamics were attributed to the absence of long-lived entanglement tubes in ring polymers, which restrict polymer relaxations in linear melts. The dynamics of NPs in ring and linear polymer melts of varying flexibility have also been recently investigated using MD [56]. That study found that NPs diffuse slightly faster in ring-polymer melts than in linear-polymer melts but exhibit the opposite behavior when the polymers were made increasingly stiff. Finally, Langevin dynamics simulations of NP transport in solutions of weakly entangled chains or rings revealed that NP diffusion is similar in both cases when the NP is smaller than the tube diameter, consistent with the similar Rouse dynamics of the two systems on these length scales [57]. Larger NPs, however, diffuse faster in solutions of ring polymers than in solutions of linear polymers.

These previous computational studies of NP diffusion in linear and ring polymers have focused on concentrated entangled systems, attributing many of the observed trends to the different entanglement behavior of the two polymer architectures. In the (semi)dilute limit where the polymers are not entangled, by contrast, solvent-mediated hydrodynamic interactions (HI) play a role in dictating how dynamics are affected by chain architecture [58–61]. Ring polymers, for example, diffuse faster in solution than linear chains with the same degree of polymerization due to the more compact structures and smaller hydrodynamic radii of the former [58]. Under shear, HI cause ring polymers to inflate, suppressing the strong tumbling motions observed for polymers with open-ended architectures such as linear chains and stars [61]. As a result, it is expected that HI may influence the dynamic coupling between NPs and polymers with different architectures.

Here, we use hybrid MD-multiparticle collision dynamics (MD–MPCD) simulations to probe the dynamics of NPs in semidilute solutions of unentangled ring polymers. We find that the dynamic coupling of the suspended NPs to the ring polymers is similar to the coupling between NPs and linear polymers if the solutions have the same monomer concentration. The terminal diffusivities of NPs in both linear- and ring-polymer solutions follow the prediction from polymer coupling theory (PCT) [16], suggesting that the long-time NP dynamics couple to polymer segmental relaxations. By contrast, in both solutions, the subdiffusive dynamics of the NPs are tightly coupled to those of the polymer centers-of-mass (COM). Finally, the addition of a large number of ring concatenation defects does not significantly modify NP dynamics.

II. METHODS

Simulations of the NP–polymer solutions were performed using an implementation of the hybrid MD–MPCD algorithm [62–64] in LAMMPS (ver. 22Aug18) [65]. Model parameters and physical quantities from the simulations were non-dimensionalized using fundamental units σ, m, ε, and $\tau = \sqrt{m\sigma^2/\varepsilon}$ for length, mass, energy, and time, respectively. In the following, we will omit these units for brevity. Details of the model systems and MD–MPCD simulations closely follow those of our recent studies of NP transport in solutions of flexible and semiflexible linear polymer chains [25,26].

Nanoparticles were modeled as smooth spheres with diameter $\sigma_{NP} = 5$, and polymers were described using a Kremer–Grest-like model [66] with monomer diameter $\sigma_P = 1$. Excluded volume interactions were included via the shifted Weeks–Chandler–Andersen potential [67],

$$U_{sWCA}(r_{ij}) = \begin{cases} 4\left[\left(\frac{\sigma_{ij}}{r_{ij}-\Delta_{ij}}\right)^{12} - \left(\frac{\sigma_{ij}}{r_{ij}-\Delta_{ij}}\right)^{6}\right] + 1, & r_{ij} \le r_{ij}^c, \\ 0, & r_{ij} > r_{ij}^c, \end{cases} \tag{1}$$

where r_{ij} is the distance between the centers of particles i and j. Parameter choices $\{\sigma_{ij}, \Delta_{ij}\} = \{\sigma_{NP}, 0\}$, $\{\sigma_P, 0\}$, and $\{\sigma_P, (\sigma_{NP} - \sigma_P)/2\}$ were used for NP–NP, polymer (P) monomer–monomer, and NP–monomer interactions, respectively. A cutoff distance of $r_{ij}^c = 2^{1/6}\sigma_{ij}$ was used to make all interactions purely repulsive.

Spring-like bonds between adjacent monomers were modeled using the finitely extensible nonlinear elastic

(FENE) potential [68],

$$U_{\mathrm{FENE}}(r_{ij}) = \begin{cases} -\frac{1}{2}kr_0^2 \ln\left[1 - \frac{r_{ij}^2}{r_0^2}\right], & r_{ij} < r_0, \\ \infty, & r_{ij} \geq r_0, \end{cases} \quad (2)$$

where $k = 30$ is the spring constant and $r_0 = 1.5$ is the maximum bond extension length. A bending potential was applied to introduce polymer stiffness [30,31,69–73]

$$U_{\mathrm{bend}}(\Theta_{ijk}) = \kappa(1 - \cos\Theta_{ijk}), \quad (3)$$

where Θ_{ijk} is the angle formed by three adjacent monomers i, j, and k ($\Theta_{ijk} = 0$ when the monomers are colinear), and κ controls the potential strength and hence polymer stiffness. Following seminal studies comparing the behavior of linear and ring polymer melts [30,31], the simulations were performed using $\kappa = 1.5$ to model highly flexible polymers.

All simulations were performed in a periodic, cubic simulation box with edge length $L_{\mathrm{box}} = 64$ (Fig. 1). We set the number of monomers per polymer N_{m} to 70 and 42 for the ring and linear polymers, respectively, which yields approximately the same radius of gyration $R_{\mathrm{g},0} \approx 5.0$ at infinite dilution. This $R_{\mathrm{g},0}$ is comparable to the diameters of the NPs used in our simulations. The number of linear polymers N_{c} was varied from 100 to 3000, achieving reduced concentrations c/c^* ranging from 0.2 to 6.0, where $c^* = 3N_{\mathrm{m}}/(4\pi R_{\mathrm{g},0}^3)$ is the overlap concentration. Similarly, the number of ring polymers was varied from 100 to 2000, spanning concentrations c/c^* from 0.2 to 4.0. In addition to studying defect-free ring polymer solutions, we also explored NP dynamics in solutions of concatenated rings in which $n_{\mathrm{linked}} = 2$, 3, or 4 ring polymers were linked in chain-like configurations. The fraction of linked rings f was varied from 0.1 to 0.5, which exceed the maximum concentration and number of concatenation impurities predicted in the typical synthesis of cyclic polymers [74].

All simulations were performed at a reduced temperature $T = 1$, using a velocity-Verlet scheme with a time step of 0.005 to integrate the equations of motion for the NPs and polymers. The systems were first equilibrated by running Langevin dynamics for a period of 2×10^5 time units, applying LAMMPS "damp" parameters of 3.0 and 0.9 (units of time) for the NPs and monomers, respectively. This duration was found to be sufficient to ensure equilibration at all conditions examined and is approximately 20× longer than the end-to-end polymer relaxation time for linear chains at the highest concentration studied ($c/c^* = 6.0$).

Following equilibration, the NP–polymer solutions were simulated for an additional period of 3×10^5 time units using a hybrid MD–MPCD scheme [25,26] to incorporate solvent-mediated HI. The MD–MPCD scheme (thermostat, solvent parameters, collision and coupling schemes, etc.) is identical to that reported in [25], and details will be omitted here for brevity. The employed parametrization results in an MPCD solvent with Schmidt number $\mathrm{Sc} \approx 12.0$ and dynamic viscosity $\eta_{\mathrm{s}} \approx 4.0$. Three independent MD–MPCD simulations (each with 20 NPs) were run for each solution and statistical quantities were computed by averaging over the resulting 60 NP trajectories.

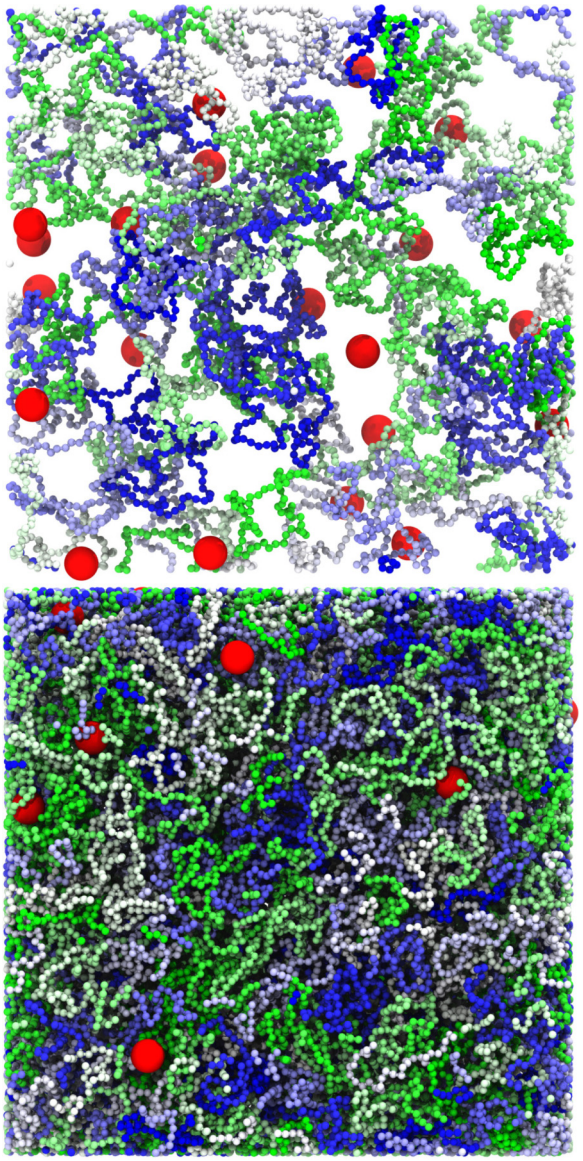

FIG. 1. Nanoparticles (large red spheres) in solutions of ring polymers (chains of small spheres) at reduced concentrations c/c^* of 0.2 (top) and 1.5 (bottom). Snapshots rendered using Visual Molecular Dynamics 1.9.3 [75].

III. RESULTS AND DISCUSSION

A. NP dynamics in linear and ring polymers

From the MD–MPCD simulations, we calculated mean-squared displacements (MSDs, $\langle \Delta r^2 \rangle$) of the individual monomers, of the polymer COM, and of the NPs for both the ring and linear polymer solutions (Fig. 2). From these MSDs, we observe important qualitative behaviors about polymer dynamics and NP transport. Similar to the behavior of linear polymers, the segmental dynamics of the rings are Zimm-like at low polymer concentrations, as indicated by the $t^{2/3}$ scaling of the monomer MSDs at early times [Fig. 2(a)]. The eventual crossover to $t^{1/2}$ scaling at higher c indicates that Rouse dynamics are recovered as HI are screened. Additionally, the MSDS of the polymer COM and NPs both

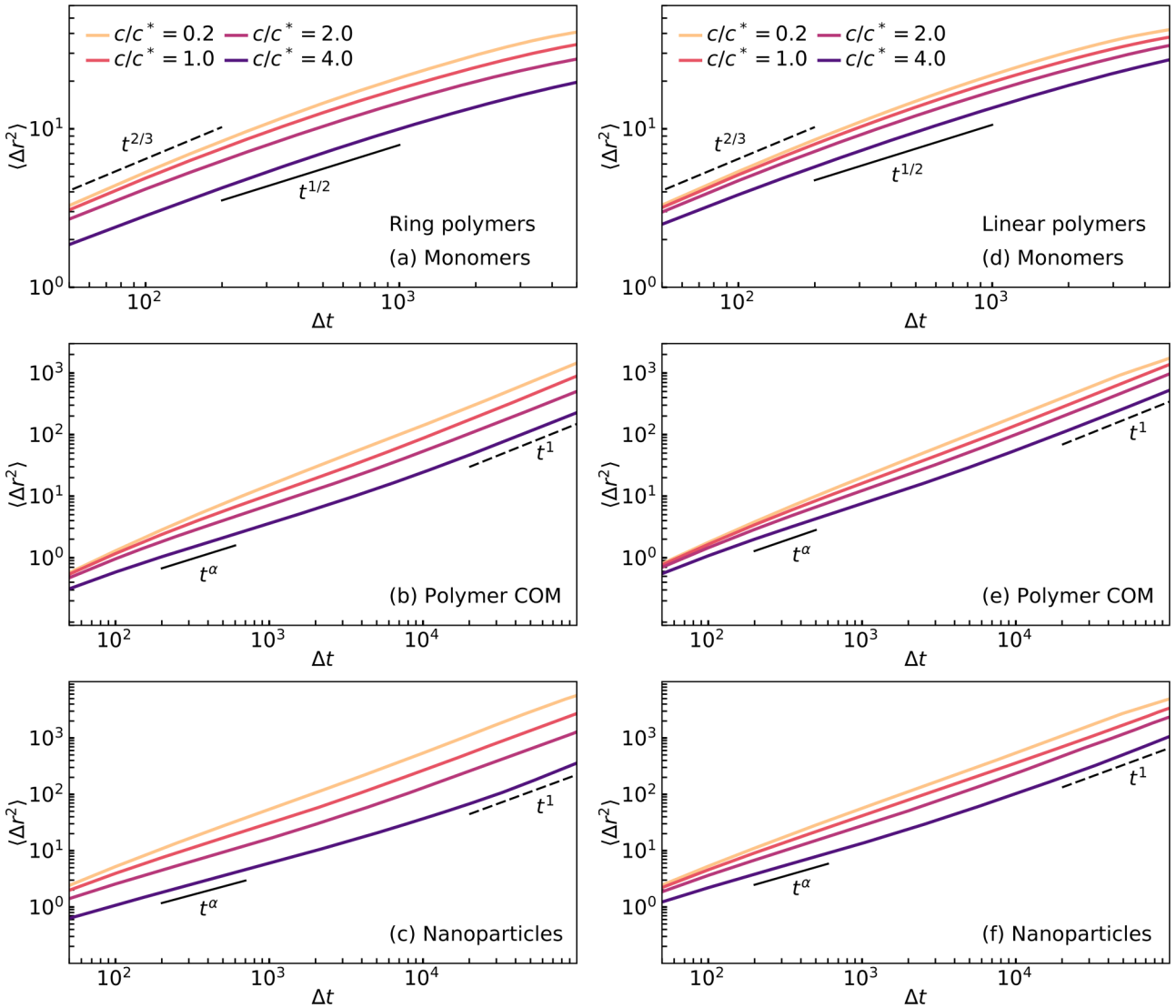

FIG. 2. Mean-squared displacements $\langle \Delta r^2 \rangle$ as functions of lag time Δt in solutions of ring polymers for (a) monomers in the polymer COM reference frame, (b) polymer COM, and (c) NPs. Dashed and solid reference lines in (a) represent Zimm ($\sim t^{2/3}$) and Rouse dynamics ($\sim t^{1/2}$), respectively. Dashed and solid reference lines in (b) and (c) indicate diffusive ($\sim t$) and subdiffusive ($\sim t^\alpha$, $\alpha < 1$) behavior, respectively. (d)–(f) Same as (a)–(c), respectively, but for solutions of linear polymers.

exhibit subdiffusive dynamics ($\langle \Delta r^2 \rangle \sim t^\alpha$ with $\alpha < 1$) at early times before crossing over to terminal diffusive behavior ($\langle \Delta r^2 \rangle \sim t$) on longer time scales [Figs. 2(b) and 2(c)]. No significant qualitative differences are observed between the MSDs computed in solutions of ring and linear polymers [Figs. 2(d)–2(f)]. This finding is similar to that from previous Langevin dynamics simulations [57], which showed that the dynamics in systems of ring and weakly entangled linear polymers are similar on length scales shorter than the entanglement length of the linear polymers.

The magnitudes of the MSDs of the monomers, polymer COM, and NPs in both systems decrease as the reduced concentration c/c^* increases, reflecting slower overall dynamics in more concentrated solutions. Note that for a given c/c^*, the dynamics in the ring-polymer solution are slower than those in the linear-polymer solution due to the higher monomer concentration c required to achieve ring overlap. Despite having the same $R_{g,0}$, the rings contain more monomers per polymer than their linear counterparts, and hence yield solutions with higher monomer concentrations at the same c/c^*. The higher monomer concentrations frustrate relaxation, leading to slower dynamics in the ring-polymer solutions. When this difference is accounted for by comparing the ring-polymer and linear-polymer solutions at the same monomer concentration c, however, the monomer and NP dynamics in both solutions are nearly indistinguishable (Fig. 3). These findings are in line with recent MD–MPCD simulations [41] that reported similar zero-shear viscosities for (semi)dilute solutions of fully flexible ring polymers, linear polymers, and their mixtures at the same monomer concentration c. A direct comparison of the MSDs (Fig. 3) reveals subtle differences between the dynamics of the polymer COM at the lower c examined, where the MSD of the linear polymer COM is slightly larger than that of the ring polymer. This result is in agreement with earlier simulations of linear and ring polymers in dilute solutions, which showed that the

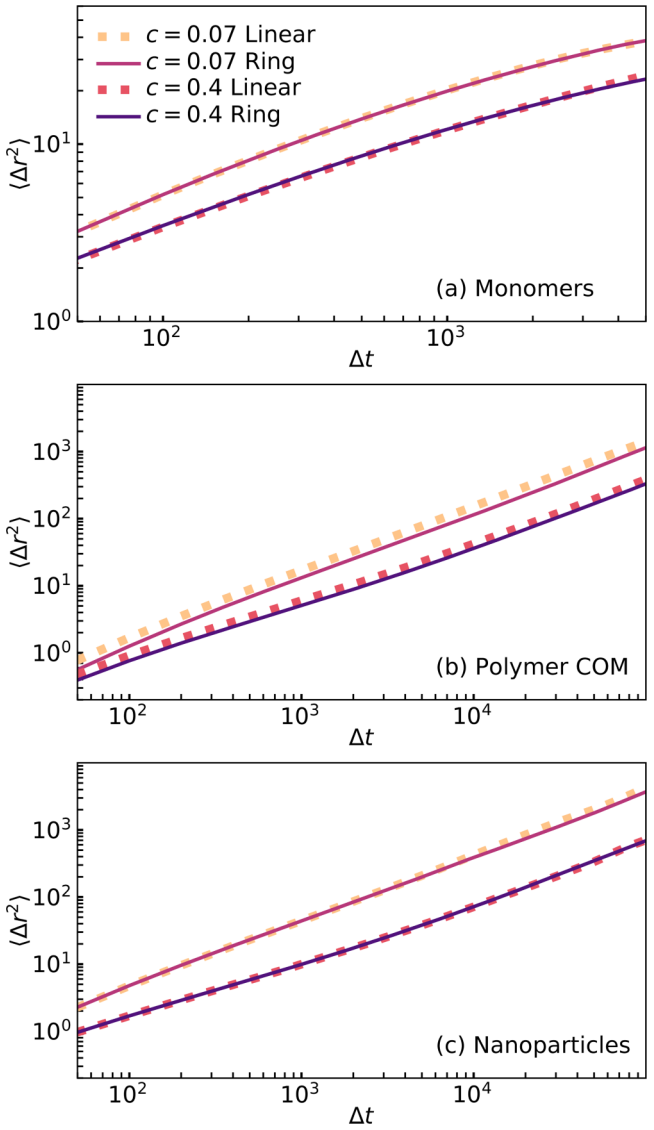

FIG. 3. Comparison of mean-squared displacement $\langle \Delta r^2 \rangle$ in solutions of ring and linear polymers (solid and dotted lines, respectively) with the same monomer concentrations c for (a) monomers in the polymer COM reference frame, (b) polymer COM, and (c) NPs.

diffusivity of a linear polymer was slightly greater (ca. 20%) than that of a ring polymer of the same R_g [58].

The presence of a subdiffusive regime in the NP MSDs suggests that the NP dynamics are coupled to those of the polymer. PCT [16] assumes that nearby polymer segments present an infinite energy barrier to NP diffusion. As a result, NPs are not able to escape the local cage created by surrounding polymers until the polymer chains relax. According to this picture, the terminal diffusivities of NPs depend on the relaxation of the polymer matrix and scale as a power-law function of the NP diameter to polymer matrix mesh size ratio: $D/D_0 \sim (\sigma_{NP}/\xi)^{-2}$, where ξ is the polymer mesh size and D_0 is the diffusivity in the background solvent. To test this prediction, we computed D_0 from simulations of NPs in the MPCD solvent. The mesh size ξ is usually taken as the blob size from scaling theory [76] or from the monomer concentration correlation length [76–78]. As discussed in [79], however, the former approach only gives an order of magnitude estimate ξ, preventing precise comparisons between systems with different chain architectures. Furthermore, the latter approach breaks down at high monomer concentrations, predicting an unphysical increase in the mesh size with c for $c \gtrsim 0.3$ (the upper end of the monomer concentration range examined here).

Thus, as suggested in [79], we instead computed ξ from the geometric pore size distribution defined by Gelb and Gubbins [80]. The local pore size $h(\mathbf{r})$ at point $\mathbf{r}$ is equal to the diameter of the largest sphere that can cover the point without overlapping with the matrix. This definition yields the total pore volume encompassed by the Connolly (reentrant) surface [79–81], and it has been widely adopted in the study of porous materials. Importantly, it provides an unambiguous geometric definition of pore size consistent with intuition for ordered materials (e.g., regular polymer networks [79]), while also being applicable to amorphous matrices [80,82]. We calculated $h(\mathbf{r})$ for polymer solutions without NPs using the algorithm described in [79,83] and defined the mesh size ξ as the spatial average of this function. In calculating the pore size, points within a distance of 0.5 of a monomer center were considered overlapping with the matrix and hence as part of its excluded volume. With this definition of ξ, we can quantitatively compare the dynamic behavior of NPs in solutions of linear and ring polymers using PCT.

In our previous study [25], we found that the PCT scaling prediction for D/D_0 is obeyed in solutions of flexible linear chains for $\sigma_{NP}/\xi \gtrsim 1$. For the solutions of flexible rings and linear polymers studied here, we observe a similar crossover of D/D_0 to the predicted PCT scaling for $\sigma_{NP}/\xi \gtrsim 1$, independent of polymer architecture (Fig. 4). The collapse of the D/D_0 values onto a single curve also reveals that, for a given size ratio σ_{NP}/ξ, the values of the long-time diffusivities are similar in the linear and ring polymer solutions. Thus, the NP dynamics in polymer solutions are nearly agnostic to the topological difference between ring and linear polymers of these sizes. Instead, NP dynamics depend strongly on the segmental relaxations of polymer chains, controlled by the mesh size ξ.

Because all of the calculations are performed using NPs of the same size, the ratio σ_{NP}/ξ is varied across different simulations by changing ξ through the polymer concentration [Fig. 4(c)]. Normalizing the dynamics by the size ratio σ_{NP}/ξ appears to account for the competing effects of faster segmental dynamics [48] but larger N_m of the ring polymers. The ring-polymer and linear-polymer solutions considered here have the same monomer concentration for a given σ_{NP}/ξ (Fig. 4). Under such conditions, the ring polymers are expected to relax faster than linear polymers with the same number of monomers N_m due to the absence of free chain ends [35]. The relaxation time, however, is also a function of the chain contour length, and in our simulations the ring polymers contain more monomers than the linear chains (N_m is 70 and 42 for the ring and linear polymers, respectively). As the MSDs suggest (Fig. 3), however, these two competing effects (i.e., polymer architecture and chain length) largely offset each other, resulting in comparable segmental relaxation times and ultimately similar NP diffusivities in solutions

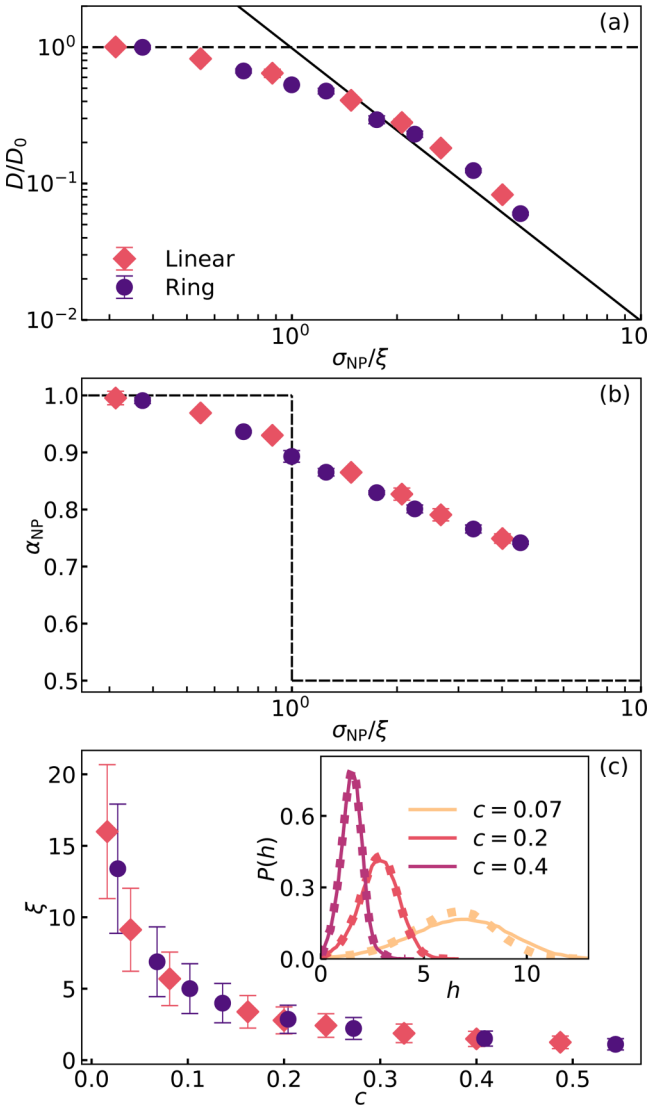

FIG. 4. (a) Normalized NP diffusivity D/D_0 in solutions of ring (circles) and linear (diamonds) polymers as a function of size ratio σ_{NP}/ξ. The solid line is the predicted scaling from PCT [16], and the dashed line indicates the diffusivity of NPs in a pure solvent (D_0). (b) Subdiffusive exponents α_{NP} of NPs as functions of size ratio σ_{NP}/ξ in solutions of ring (circles) and linear (diamonds) polymers. The dashed lines are the prediction from PCT [16]. (c) Mesh size ξ as a function of monomer concentration c for ring (circles) and linear (diamonds) polymer solutions. Uncertainties in ξ are the standard deviation of the pore size distribution at each concentration. Inset to (c) shows the pore size distributions for the ring and linear polymer solutions (solid and dotted lines, respectively) at three representative monomer concentrations; the mesh size is the first moment of the pore size distribution, i.e., $\xi \equiv \int hP(h)dh$.

of rings or linear polymers with similar monomer concentrations and mesh sizes. This similarity between NP dynamics in ring and linear polymers is consistent with the PCT assumption that NPs feel only a local viscosity equal to that of a solution of effective polymer chains with a characteristic radius $R_{eff} = \sigma_{NP}/2$ [16]. Because the ring and linear polymers are both larger than the NPs in our simulations, the observed NP dynamics are insensitive to polymer topology.

PCT also predicts that the subdiffusive exponent for the NPs (α_{NP}) should abruptly decrease from 1 to 0.5 at $\sigma_{NP}/\xi = 1$ due to complete coupling of the NPs with the polymer segmental relaxations. Indeed, experiments show that an exponent of 0.5 is measured when NPs are chemically bonded to a polymer network [84]. Moreover, our simulations (not shown) also reveal that the NP dynamics are purely diffusive in solutions of free (unpolymerized) monomers over similar ranges of c, with NP diffusion coefficients systematically larger than in the corresponding polymer solutions. Thus, the NP subdiffusive dynamics arise from coupling with polymer segmental relaxations, leading to an exponent of 0.5 when complete coupling occurs. In accord with our previous simulation studies [25,26] and experiments [15], however, we observe that the short-time NP dynamics in both the ring-polymer and linear-polymer solutions deviate from PCT predictions (Fig. 4). Rather than abruptly changing, the subdiffusive exponents gradually decay as the size ratio σ_{NP}/ξ increases. Moreover, as with the long-time diffusivities, the close numerical agreement between α_{NP} in the ring and linear polymer solutions suggests that the subdiffusive dynamics are insensitive to differences between the two polymer architectures (i.e., free chain ends) for the chain sizes and range of σ_{NP}/ξ examined in this study.

We also analyzed the subdiffusive exponents of the polymer COM (α_P) and compared them to those of the NPs (α_{NP}) as a function of c/c^* (Fig. 5). Both α_P and α_{NP} exhibit a similar concentration dependence, suggesting a tight coupling between the subdiffusive dynamics of the NPs and

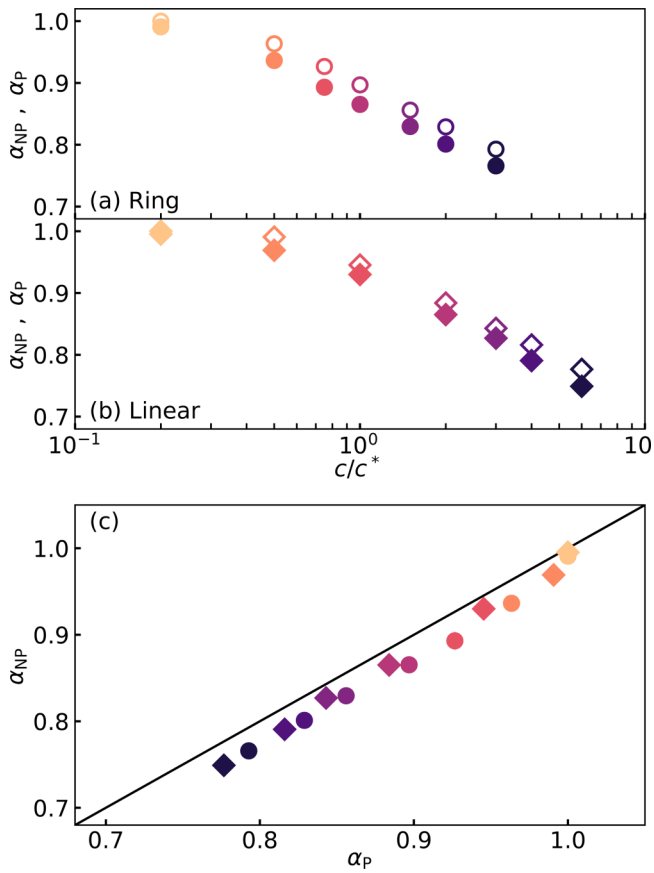

FIG. 5. (a) and (b) Subdiffusive exponents for the NPs (α_{NP}, closed symbols) and polymer COM (α_P, open symbols) in solutions of (a) ring (circles) and (b) linear (diamonds) polymers, as functions of the reduced polymer concentration c/c^*. (c) α_{NP} as a function of α_P. The solid line indicates $\alpha_{NP} = \alpha_P$.

polymer COM, which is consistent with our previous findings for solutions of flexible linear polymers [25]. Moreover, the observation that $\alpha_{NP} \simeq \alpha_P$ [Fig. 5(c)] indicates that the degree of coupling of NP dynamics to those of the polymer COM on short time scales is similar in both systems and remarkably insensitive to differences in the two polymer architectures.

By contrast, in our analogous study of semiflexible linear chains, we observed a decoupling of α_{NP} and α_P as the chain stiffness was increased and the polymers became increasingly rod-shaped [26]. The segmental dynamics of the linear polymers dramatically slowed down and the polymer COM diffusion became increasingly anisotropic on the time scales relevant to the subdiffusive motion of the NPs, altering the way in which polymers and NPs dynamically couple on short times. This contrast of NP dynamics in solutions of semiflexible chains and solutions of ring polymers suggests that relaxations controlled by polymer flexibility may more strongly affect NP dynamics than those controlled by free chain ends.

B. Effect of ring concatenation

Ring polymers can also form concatenated structures in which one or more rings interlock, imposing permanent topological constraints that may influence their properties [51,52,76,85,86]. Indeed, interlocked ring structures are found in natural polymers such as mitochondrial DNA [86,87] and emerge as impurities during the production of synthetic ring polymers [88]. Additionally, strategies have been recently developed to purposefully synthesize high molecular weight concatenated chains, known as poly[n]catenanes, that consist of tens of interlocking rings [85]. Rouse mode analysis of isolated poly[n]catenane shows that concatenation leads to a slowdown of relaxations over short length scales, resembling the effects of entanglement on linear polymers [89]. Relaxations over longer length scales, however, remain largely unperturbed and similar to those of unentangled linear polymers [89]. In ring polymer melts, concatenation leads to changes in the structure on short and intermediate length scales associated with local density inhomogeneities along the polymer contour [51] and a significant slowing down of the segmental dynamics on short length scales [52], similar to that observed in dilute systems [89]. Although the structure and dynamics of dilute solutions and concentrated melts of concatenated rings have been previously investigated, their behavior in the semidilute regime remains incompletely understood. Furthermore, it is unclear how ring concatenation will affect the NP–polymer coupling, due to the potential slowing down of the polymer dynamics.

Consequently, we examined the effect of ring concatenation on the short- and long-time dynamics of polymers and NPs at an intermediate monomer concentration of $c = 0.2$. As the fraction of concatenated rings in the system f is increased, the MSDs of the monomers in the ring COM reference frame decrease slightly [Fig. 6(a)] but exhibit no discernible dependence on n_{linked} (not shown). Similarly, the short-time subdiffusive exponent α_P of the ring COM decreases slightly with increasing f [see Figs. 6(b) and 7].

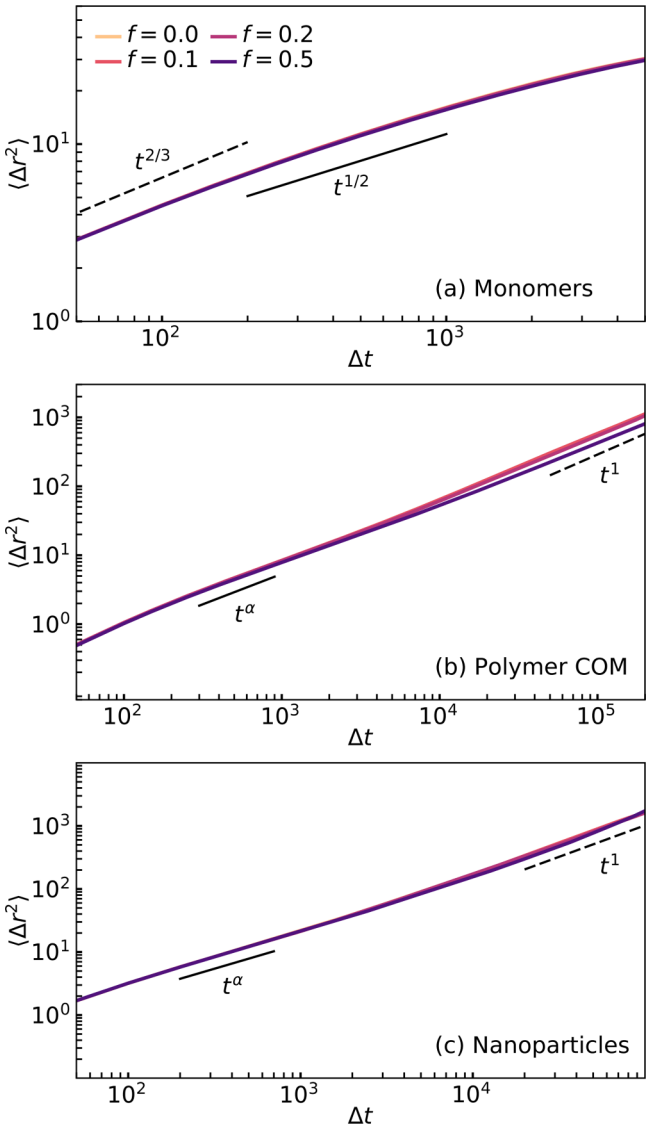

FIG. 6. Mean-squared displacements $\langle \Delta r^2 \rangle$ as functions of lag time Δt for (a) monomers in the polymer COM reference frame, (b) polymer COM, and (c) NPs in solutions of ring polymers containing various fractions f of concatenated rings with a monomer concentration of $c = 0.2$. The concatenated rings are linked in chain-like structures consisting of $n_{linked} = 3$ rings per chain. Dashed and solid reference lines in (a) represent Zimm ($\sim t^{2/3}$) and Rouse dynamics ($\sim t^{1/2}$), respectively. Dashed lines and solid reference lines in (b) and (c) indicate diffusive ($\sim t$) and subdiffusive ($\sim t^{\alpha}$, $\alpha < 1$) behavior, respectively.

Interestingly, this behavior is independent of the number of linked rings in each chain n_{linked}. These observations suggest that over the range of parameters studied here, concatenation results in an almost negligible suppression of the polymer short-time dynamics in semidilute solutions. By contrast, the MSD for the ring COM at long times (Fig. 6), and hence the long-time diffusivity $D_P/D_{0,P}$ (Fig. 7), decreases as f and n_{linked} increase, reflecting the constrained motion of the individual polymers and increased hydrodynamic radius of the concatenated rings [52].

The behavior of the short-time NP subdiffusive exponent α_{NP} closely follows that of α_P, indicating that the motions of the NPs and ring COM remain tightly coupled on short time scales, independent of f and n_{linked}. Moreover, the long-time

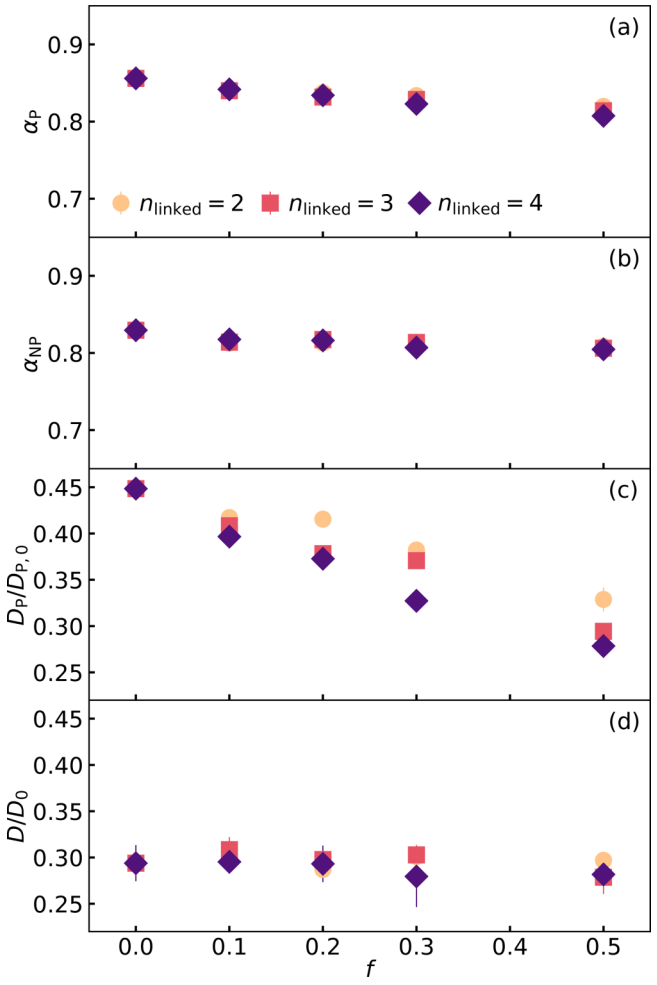

FIG. 7. (a) Polymer COM subdiffusive exponent α_P, (b) NP subdiffusive exponent α_{NP}, (c) reduced polymer COM diffusivity $D_P/D_{P,0}$, and (d) reduced NP diffusivity D/D_0 as functions of the fraction of concatenated rings f for systems with a monomer concentration of $c = 0.2$. Circles, squares, and diamonds denote systems in which ring polymers are concatenated in chain-like structures containing $n_{linked} = 2$, 3, or 4 rings, respectively. $D_{P,0}$ is the diffusivity of polymer COM at the lowest concentration studied ($c/c^* = 0.2$, $c = 0.27$), and D_0 is the NP diffusivity in a pure solvent.

NP diffusivity D/D_0 remains nearly constant as f and n_{linked} are varied. This result is consistent with PCT, which predicts that the NP's terminal diffusive motions are controlled predominately by local polymer segmental relaxations (Fig. 6), which appear largely unaffected by concatenation. Hence, for the conditions examined here, we do not find that the constraints imposed by ring interlocking strongly influence segmental relaxations or NP dynamics.

Note that we have investigated the dynamics of mixtures of concatenated and nonconcatenated rings, averaging over all rings in the solution to characterize segmental relaxations. It is possible that changes in the segmental dynamics may become more pronounced in solutions with larger fractions of concatenated rings, higher densities, and/or longer concatenated chains, as suggested by previous simulations of melts [52], and thereby more significantly affect NP transport. Although this topic merits additional investigation in future studies, a necessary first step will be understanding the effects of concatenation on the structure and dynamics of bulk semidilute ring solutions, which to our knowledge, remains largely unexplored.

IV. CONCLUSIONS

Using hybrid MD–MPCD simulations, we investigated the diffusion of NPs in semi-dilute solutions of ring and linear polymers. For these two architectures, we found that the dynamics of the monomers, the polymer COM, and the NPs are nearly identical when solutions at the same monomer concentration are compared. On long time scales, the normalized diffusivities of NPs in ring-polymer and linear-polymer solutions follow the predictions of PCT [16]. On short time scales, the subdiffusive exponents of the NPs closely track those of the polymer COM in both ring-polymer and linear-polymer solutions, insensitive to the differences in the two polymer architectures. As with predictions from any theoretical or computational study, however, experiments are needed to validate these findings and in particular show that they hold in systems with polymers that are significantly larger than those than can be easily explored in simulation. Whether PCT predictions hold for other polymer architectures (e.g., stars and dendrimers), systems with topological constraints such as knots, or mixtures of linear chains and rings, which are reported to exhibit distinct dynamical properties [40], also remains an open question that will require further investigation. Finally, we showed that increasing the fraction of concatenated rings leads to a slight decrease in the subdiffusive exponents of NPs and polymer COM, which closely track each other, but the long-time diffusivity remains nearly constant. In the context of PCT, which predicts that NP diffusive motions couple to segmental relaxations, the latter finding is surprising, given that recent studies have shown that concatenation slows these relaxations in melts [52]. Understanding of the effects of concatenation on the dynamics of bulk ring polymer solutions remains limited, however, and will require future study to fully rationalize this result.

AUTHORS' CONTRIBUTION

R.C. and S.B.K. contributed equally to this work.

ACKNOWLEDGMENTS

This work was supported by the Welch Foundation [Grant Nos. E-1882 (JCP) and E-1869 (JCC)] and the National Science Foundation (Nos. CBET-1751173 and CBET-1803728). A.N. received support from the German Research Foundation (DFG) under Project Nos. NI 1487/2-1 and NI 1487/2-2. Computational resources were provided by the Hewlett Packard Enterprise Data Science Institute at the University of Houston and the Texas Advanced Computing Center at the University of Texas at Austin.

REFERENCES

[1] Hanemann, T., and D. V. Szabó, "Polymer-nanoparticle composites: From synthesis to modern applications," Materials **3**, 3468–3517 (2010).

[2] Chen, Q., S. Gong, J. Moll, D. Zhao, S. K. Kumar, and R. H. Colby, "Mechanical reinforcement of polymer nanocomposites from percolation of a nanoparticle network," ACS Macro Lett. **4**, 398–402 (2015).
[3] Sarkar, B., and P. Alexandridis, "Block copolymer-nanoparticle composites: Structure, functional properties, and processing," Prog. Polym. Sci. **40**, 33–62 (2015).
[4] Shamsijazeyi, H., C. A. Miller, M. S. Wong, J. M. Tour, and R. Verduzco, "Polymer-coated nanoparticles for enhanced oil recovery," J. Appl. Polym. Sci. **131**, 040576 (2014).
[5] Soppimath, K. S., T. M. Aminabhavi, A. R. Kulkarni, and W. E. Rudzinski, "Biodegradable polymeric nanoparticles as drug delivery devices," J. Control. Release **70**, 1–20 (2001).
[6] Liechty, W. B., D. R. Kryscio, B. V. Slaughter, and N. A. Peppas, "Polymers for drug delivery systems," Annu. Rev. Chem. Biomol. Eng. **1**, 149–173 (2010).
[7] Tang, L., X. Yang, Q. Yin, K. Cai, H. Wang, I. Chaudhury, C. Yao, Q. Zhou, M. Kwon, J. A. Hartman, I. T. Dobrucki, L. W. Dobrucki, L. B. Borst, S. Lezmi, W. G. Helferich, A. L. Ferguson, T. M. Fan, and J. Cheng, "Investigating the optimal size of anticancer nanomedicine," Proc. Natl. Acad. Sci. U.S.A. **111**, 15344–15349 (2014).
[8] Blanco, E., H. Shen, and M. Ferrari, "Principles of nanoparticle design for overcoming biological barriers to drug delivery," Nat. Biotechnol. **33**, 941–951 (2015).
[9] Mason, T. G., and D. A. Weitz, "Optical measurements of frequency-dependent linear viscoelastic moduli of complex fluids," Phys. Rev. Lett. **74**, 1250 (1995).
[10] Mason, T. G., T. Gisler, K. Kroy, E. Frey, and D. A. Weitz, "Rheology of F-actin solutions determined from thermally driven tracer motion," J. Rheol. **44**, 917–927 (2000).
[11] Ye, X., P. Tong, and L. J. Fetters, "Transport of probe particles in semidilute polymer solutions," Macromolecules **31**, 5785–5793 (1998).
[12] Cheng, Y., R. K. Prud'homme, and J. L. Thomas, "Diffusion of mesoscopic probes in aqueous polymer solutions measured by fluorescence recovery after photobleaching," Macromolecules **35**, 8111–8121 (2002).
[13] Tuteja, A., M. E. Mackay, S. Narayanan, S. Asokan, and M. S. Wong, "Breakdown of the continuum Stokes-Einstein relation for nanoparticle diffusion," Nano Lett. **7**, 1276–1281 (2007).
[14] Kohli, I., and A. Mukhopadhyay, "Diffusion of nanoparticles in semidilute polymer solutions: Effect of different length scales," Macromolecules **45**, 6143–6149 (2012).
[15] Poling-Skutvik, R., R. Krishnamoorti, and J. C. Conrad, "Size-dependent dynamics of nanoparticles in unentangled polyelectrolyte solutions," ACS Macro Lett. **4**, 1169–1173 (2015).
[16] Cai, L.-H., S. Panyukov, and M. Rubinstein, "Mobility of nonsticky nanoparticles in polymer liquids," Macromolecules **44**, 7853–7863 (2011).
[17] Egorov, S. A., "Anomalous nanoparticle diffusion in polymer solutions and melts: A mode-coupling theory study," J. Chem. Phys. **134**, 084903 (2011).
[18] Dell, Z. E., and K. S. Schweizer, "Theory of localization and activated hopping of nanoparticles in cross-linked networks and entangled polymer melts," Macromolecules **47**, 405–414 (2014).
[19] Cai, L.-H., S. Panyukov, and M. Rubinstein, "Hopping diffusion of nanoparticles in polymer matrices," Macromolecules **48**, 847–862 (2015).
[20] Dong, Y., X. Feng, N. Zhao, and Z. Hou, "Diffusion of nanoparticles in semidilute polymer solutions: A mode-coupling theory study," J. Chem. Phys. **143**, 024903 (2015).
[21] Kalathi, J. T., G. S. Grest, and S. K. Kumar, "Universal viscosity behavior of polymer nanocomposites," Phys. Rev. Lett. **109**, 198301 (2012).
[22] Kalathi, J. T., U. Yamamoto, K. S. Schweizer, G. S. Grest, and S. K. Kumar, "Nanoparticle diffusion in polymer nanocomposites," Phys. Rev. Lett. **112**, 108301 (2014).
[23] Chen, A., N. Zhao, and Z. Hou, "The effect of hydrodynamic interactions on nanoparticle diffusion in polymer solutions: A multi-particle collision dynamics study," Soft Matter **13**, 8625–8635 (2017).
[24] Sorichetti, V., V. Hugouvieux, and W. Kob, "Structure and dynamics of a polymer-nanoparticle composite: Effect of nanoparticle size and volume fraction," Macromolecules **51**, 5375–5391 (2018).
[25] Chen, R., R. Poling-Skutvik, A. Nikoubashman, M. P. Howard, J. C. Conrad, and J. C. Palmer, "Coupling of nanoparticle dynamics to polymer center-of-mass motion in semidilute polymer solutions," Macromolecules **51**, 1865–1872 (2018).
[26] Chen, R., R. Poling-Skutvik, M. P. Howard, A. Nikoubashman, S. A. Egorov, J. C. Conrad, and J. C. Palmer, "Influence of polymer flexibility on nanoparticle dynamics in semidilute solutions," Soft Matter **15**, 1260–1268 (2019).
[27] Brown, S., and G. Szamel, "Structure and dynamics of ring polymers," J. Chem. Phys. **108**, 4705–4708 (1998).
[28] Gagliardi, S., V. Arrighi, A. Dagger, and A. Semlyen, "Conformation of cyclic and linear polydimethylsiloxane in the melt: A small-angle neutron-scattering study," Appl. Phys. A **74**, s469–s471 (2002).
[29] Beaucage, G., and A. S. Kulkarni, "Dimensional description of cyclic macromolecules," Macromolecules **43**, 532–537 (2009).
[30] Halverson, J. D., W. B. Lee, G. S. Grest, A. Y. Grosberg, and K. Kremer, "Molecular dynamics simulation study of nonconcatenated ring polymers in a melt. I. Statics," J. Chem. Phys. **134**, 204904 (2011).
[31] Halverson, J. D., W. B. Lee, G. S. Grest, A. Y. Grosberg, and K. Kremer, "Molecular dynamics simulation study of nonconcatenated ring polymers in a melt. II. Dynamics," J. Chem. Phys. **134**, 204905 (2011).
[32] Ge, T., S. Panyukov, and M. Rubinstein, "Self-similar conformations and dynamics in entangled melts and solutions of nonconcatenated ring polymers," Macromolecules **49**, 708–722 (2016).
[33] Ge, T., J. T. Kalathi, J. D. Halverson, G. S. Grest, and M. Rubinstein, "Nanoparticle motion in entangled melts of linear and nonconcatenated ring polymers," Macromolecules **50**, 1749–1754 (2017).
[34] Robertson, R. M., and D. E. Smith, "Strong effects of molecular topology on diffusion of entangled DNA molecules," Proc. Natl. Acad. Sci. U.S.A. **104**, 4824–4827 (2007).
[35] Kapnistos, M., M. Lang, D. Vlassopoulos, W. Pyckhout-Hintzen, D. Richter, D. Cho, T. Chang, and M. Rubinstein, "Unexpected power-law stress relaxation of entangled ring polymers," Nat. Mater. **7**, 997–1002 (2008).
[36] Rosa, A., E. Orlandini, L. Tubiana, and C. Micheletti, "Structure and dynamics of ring polymers: Entanglement effects because of solution density and ring topology," Macromolecules **44**, 8668–8680 (2011).
[37] Goossen, S., A. Brás, M. Krutyeva, M. Sharp, P. Falus, A. Feoktystov, U. Gasser, W. Pyckhout-Hintzen, A. Wischnewski, and D. Richter, "Molecular scale dynamics of large ring polymers," Phys. Rev. Lett. **113**, 168302 (2014).
[38] Soh, B. W., A. R. Klotz, R. M. Robertson-Anderson, and P. S. Doyle, "Long-lived self-entanglements in ring polymers," Phys. Rev. Lett. **123**, 048002 (2019).
[39] Gartner, T. E., F. M. Haque, A. M. Gomi, S. M. Grayson, M. J. A. Hore, and A. Jayaraman, "Scaling exponent and effective interactions in linear and cyclic polymer solutions: Theory, simulations, and experiments," Macromolecules **52**, 4579–4589 (2019).
[40] Zhou, Y., K.-W. Hsiao, K. E. Regan, D. Kong, G. B. McKenna, R. M. Robertson-Anderson, and C. M. Schroeder, "Effect of molecular architecture on ring polymer dynamics in semidilute linear polymer solutions," Nat. Commun. **10**, 001753 (2019).

[41] Weiss, L. B., C. N. Likos, and A. Nikoubashman, "Spatial demixing of ring and chain polymers in pressure-driven flow," Macromolecules **52**, 7858–7869 (2019).
[42] de Gennes, P.-G., "Reptation of a polymer chain in the presence of fixed obstacles," J. Chem. Phys. **55**, 572–579 (1971).
[43] McLeish, T., "Tube theory of entangled polymer dynamics," Adv. Phys. **51**, 1379–1527 (2002).
[44] Cates, M., and J. Deutsch, "Conjectures on the statistics of ring polymers," J. Phys. **47**, 2121–2128 (1986).
[45] Rubinstein, M., "Dynamics of ring polymers in the presence of fixed obstacles," Phys. Rev. Lett. **57**, 3023–3026 (1986).
[46] Nechaev, S., A. Semenov, and M. Koleva, "Dynamics of a polymer chain in an array of obstacles," Physica A **140**, 506–520 (1987).
[47] Grosberg, A. Y., S. K. Nechaev, and E. I. Shakhnovich, "The role of topological constraints in the kinetics of collapse of macromolecules," J. Phys. **49**, 2095–2100 (1988).
[48] Obukhov, S. P., M. Rubinstein, and T. Duke, "Dynamics of a ring polymer in a gel," Phys. Rev. Lett. **73**, 1263–1266 (1994).
[49] Tsolou, G., N. Stratikis, C. Baig, P. S. Stephanou, and V. G. Mavrantzas, "Melt structure and dynamics of unentangled polyethylene rings: Rouse theory, atomistic molecular dynamics simulation, and comparison with the linear analogues," Macromolecules **43**, 10692–10713 (2010).
[50] McLeish, T., "Polymer dynamics: Floored by the rings," Nat. Mater. **7**, 933–935 (2008).
[51] Rauscher, P. M., K. S. Schweizer, S. J. Rowan, and J. J. de Pablo, "Thermodynamics and structure of poly[n]catenane melts," Macromolecules **53**, 3390–3408 (2020).
[52] Rauscher, P. M., K. S. Schweizer, S. J. Rowan, and J. J. de Pablo, "Dynamics of poly[n]catenane melts," J. Chem. Phys. **152**, 214901 (2020).
[53] Rauscher, P. M., S. J. Rowan, and J. J. de Pablo, "Hydrodynamic interactions in topologically linked ring polymers," Phys. Rev. E **102**, 032502 (2020).
[54] Ahmadian Dehaghani, Z., I. Chubak, C. N. Likos, and M. R. Ejtehadi, "Effects of topological constraints on linked ring polymers in solvents of varying quality," Soft Matter **16**, 3029–3038 (2020).
[55] Ge, T., G. S. Grest, and M. Rubinstein, "Nanorheology of entangled polymer melts," Phys. Rev. Lett. **120**, 057801 (2018).
[56] Zhou, X., Y. Jiang, J. Chen, L. He, and L. Zhang, "Size-dependent nanoparticle dynamics in semiflexible ring polymer nanocomposites," Polymer **131**, 243–251 (2017).
[57] Nahali, N., and A. Rosa, "Nanoprobe diffusion in entangled polymer solutions: Linear vs unconcatenated ring chains," J. Chem. Phys. **148**, 194902 (2018).
[58] Hegde, G. A., J.-F. Chang, Y.-L. Chen, and R. Khare, "Conformation and diffusion behavior of ring polymers in solution: A comparison between molecular dynamics, multiparticle collision dynamics, and lattice boltzmann simulations," J. Chem. Phys. **135**, 184901 (2011).
[59] Hsiao, K.-W., C. M. Schroeder, and C. E. Sing, "Ring polymer dynamics are governed by a coupling between architecture and hydrodynamic interactions," Macromolecules **49**, 1961–1971 (2016).
[60] Young, C. D., J. R. Qian, M. Marvin, and C. E. Sing, "Ring polymer dynamics and tumbling-stretch transitions in planar mixed flows," Phys. Rev. E **99**, 062502 (2019).
[61] Liebetreu, M., and C. N. Likos, "Hydrodynamic inflation of ring polymers under shear," Commun. Mater. **1**, 000004 (2020).
[62] Malevanets, A., and R. Kapral, "Mesoscopic model for solvent dynamics," J. Chem. Phys. **110**, 8605–8613 (1999).
[63] Gompper, G., T. Ihle, D. M. Kroll, and R. G. Winkler, "Multi-particle collision dynamics: A particle-based mesoscale simulation approach to the hydrodynamics of complex fluids," in *Adv. Comput. Simul. Approaches Soft Matter Sci. III* (Springer, New York, 2009), pp. 1–87.
[64] Howard, M. P., A. Nikoubashman, and J. C. Palmer, "Modeling hydrodynamic interactions in soft materials with multiparticle collision dynamics," Curr. Opin. Chem. Eng. **23**, 34–43 (2019).
[65] Plimpton, S., "Fast parallel algorithms for short-range molecular dynamics," J. Comput. Phys. **117**, 1–19 (1995).
[66] Kremer, K., and G. S. Grest, "Dynamics of entangled linear polymer melts: A molecular-dynamics simulation," J. Chem. Phys. **92**, 5057–5086 (1990).
[67] Weeks, J. D., D. Chandler, and H. C. Andersen, "Role of repulsive forces in determining the equilibrium structure of simple liquids," J. Chem. Phys. **54**, 5237–5247 (1971).
[68] Bishop, M., M. H. Kalos, and H. L. Frisch, "Molecular dynamics of polymeric systems," J. Chem. Phys. **70**, 1299–1304 (1979).
[69] Nikoubashman, A., A. Milchev, and K. Binder, "Dynamics of single semiflexible polymers in dilute solution," J. Chem. Phys. **145**, 234903 (2016).
[70] Nikoubashman, A., and M. P. Howard, "Equilibrium dynamics and shear rheology of semiflexible polymers in solution," Macromolecules **50**, 8279–8289 (2017).
[71] Faller, R., A. Kolb, and F. Müller-Plathe, "Local chain ordering in amorphous polymer melts: Influence of chain stiffness," Phys. Chem. Chem. Phys. **1**, 2071–2076 (1999).
[72] Faller, R., F. Müller-Plathe, and A. Heuer, "Local reorientation dynamics of semiflexible polymers in the melt," Macromolecules **33**, 6602–6610 (2000).
[73] Faller, R., and F. Müller-Plathe, "Chain stiffness intensifies the reptation characteristics of polymer dynamics in the melt," Chem. Phys. Chem. **2**, 180–184 (2001).
[74] Fischer, J., M. Lang, and J.-U. Sommer, "The formation and structure of olympic gels," J. Chem. Phys. **143**, 243114 (2015).
[75] Humphrey, W., A. Dalke, and K. Schulten, "VMD—Visual molecular dynamics," J. Mol. Graphics **14**, 33–38 (1996).
[76] de Gennes, P.-G., *Scaling Concepts in Polymer Physics* (Cornell University, Ithaca, 1979).
[77] Rubinstein, M., and R. H. Colby, *Polymer Physics* (Oxford University, New York, 2003).
[78] Koshy, R., T. Desai, P. Keblinski, J. Hooper, and K. S. Schweizer, "Density fluctuation correlation length in polymer fluids," J. Chem. Phys. **119**, 7599–7603 (2003).
[79] Sorichetti, V., V. Hugouvieux, and W. Kob, "Determining the mesh size of polymer solutions via the pore size distribution," Macromolecules **53**, 2568–2581 (2020).
[80] Gelb, L. D., and K. E. Gubbins, "Pore size distributions in porous glasses: A computer simulation study," Langmuir **15**, 305–308 (1999).
[81] Connolly, M. L., "Analytical molecular surface calculation," J. Appl. Crystallogr. **16**, 548–558 (1983).
[82] Palmer, J. C., J. D. Moore, J. K. Brennan, and K. E. Gubbins, "Simulating local adsorption isotherms in structurally complex porous materials: A direct assessment of the slit pore model," J. Phys. Chem. Lett. **2**, 165–169 (2011).
[83] Bhattacharya, S., and K. E. Gubbins, "Fast method for computing pore size distributions of model materials," Langmuir **22**, 7726–7731 (2006).
[84] Sprakel, J., J. van der Gucht, M. A. Cohen Stuart, and N. A. M. Besseling, "Rouse dynamics of colloids bound to polymer networks," Phys. Rev. Lett. **99**, 208301 (2007).
[85] Wu, Q., P. M. Rauscher, X. Lang, R. J. Wojtecki, J. J. de Pablo, M. J. A. Hore, and S. J. Rowan, "Poly[n]catenanes: Synthesis of molecular interlocked chains," Science **358**, 1434–1439 (2017).

[86] Klotz, A. R., B. W. Soh, and P. S. Doyle, "Equilibrium structure and deformation response of 2D kinetoplast sheets," Proc. Natl. Acad. Sci. U.S.A. **117**, 121–127 (2020).

[87] Clayton, D. A., and J. Vinograd, "Circular dimer and catenate forms of mitochondrial DNA in human leukaemic leucocytes," Nature **216**, 652–657 (1067).

[88] Edwards, J. P., W. J. Wolf, and R. H. Grubbs, "The synthesis of cyclic polymers by olefin metathesis: Achievements and challenges," J. Polym. Sci. Part A: Polym. Chem. **57**, 228–242 (2019).

[89] Rauscher, P. M., S. J. Rowan, and J. J. de Pablo, "Topological effects in isolated poly[n]catenanes: Molecular dynamics simulations and Rouse mode analysis," ACS Macro Lett. **7**, 938–943 (2018).